



The XXIII International Symposium on Lepton and Photon Interactions at High Energy, LP2007

Aug 13-18, Daegu, Korea

Electronic Access: www-h1.desy.de/h1/www/publications/conf/conf_list.html

Combination of H1 and ZEUS Deep Inelastic $e^\pm p$ Scattering Cross Section Measurements

H1 and ZEUS Collaborations

Abstract

Deep inelastic scattering cross section measurements previously published by the H1 and ZEUS collaborations are combined. The procedure takes into account the systematic error correlations in a coherent approach, leading to a significantly reduced overall cross section uncertainty by cross calibrating the various data sets. The analysis is restricted to data with momentum transfers $Q^2 \geq 1.5 \text{ GeV}^2$ and the running period HERA I, specifically data taken between 1996 – 2000.

1 Introduction

In June 2007 the operation of HERA was terminated after a period of 15 years of data taking. During this time the H1 and ZEUS collaborations successfully operated their general purpose detectors which were adapted in 2001 to the luminosity upgrade of the collider interaction regions. The data taken up until 2000 have yielded the first accurate neutral and charged current (NC and CC) deep inelastic scattering cross section measurement from $\sim 115 \text{ pb}^{-1}$ of $e^\pm p$ scattering data per experiment. These data have been crucial in substantially constraining the parton density functions (PDFs) of the proton. The NC and CC data from HERA I allow a complete set of up and down quark and anti-quark distributions to be determined across the full range of Bjorken x and Q^2 covered by the measurements and in particular they allow the gluon distribution and the strong coupling constant to be determined with unique accuracy.

In a first joint analysis the H1 and ZEUS Collaborations released a set of combined neutral current data at high momentum transfers squared, Q^2 , to the ICHEP Conference in 2006 [1]. Since at high Q^2 the uncertainties were dominated by the statistical precision, the data were combined taking simple averages treating the data as uncorrelated. The physics result consisted in improved measurements of the photon- Z exchange interference as is manifest in polarisation and charge asymmetry effects in NC scattering.

In this paper the combined analysis is moved a step further by including charged current $e^\pm p$ data and the accurate low Q^2 neutral current data in the deep inelastic region. The goal of this study is to provide data of the highest possible accuracy in order to achieve precise determinations of the proton PDFs. This requires a joint consideration of data from the two collider experiments which carefully takes into account the correlations within the data as resulting from different sources of uncertainty. Since both cross section sets, from H1 and ZEUS, are supposed to represent a common truth, forcing them to agree results in a strong constraint. This is used here to cross calibrate the measurements. Since the data precision below $Q^2 \simeq 200 \text{ GeV}^2$ is limited by systematic uncertainties, the cross calibration provides a means of substantially reducing the overall uncertainty to below the simple average.

The present paper is to be seen as part of a mid term strategy. It will be followed by combinations of even more accurate data, from both HERA operation periods I and II, and by joint pQCD analyses at high orders which will significantly improve the results from HERA, both for the understanding of strong interaction dynamics governing the structure of the proton and for predictions of pp scattering processes at higher energies at the LHC.

The paper is organised as follows. Section 2 gives an overview on the current treatment of data and their uncertainties in modern QCD fit analyses. Section 3 introduces the combination method used to obtain combined HERA data. The input data and adapted analysis procedure are discussed in Section 4 as well as a discussion of additional uncertainties arising from the combination procedure. Results based on HERA I NC and CC data are shown in Section 5.

2 Data Handling in Parton Distribution Analyses

Deep inelastic cross sections in NC and CC scattering are the most complete basis for the extraction of parton distributions which, by applying factorisation arguments, are used for the

description of partonic interactions in other particle collisions. In the previous two decades analyses have been developed which, using QCD evolution equations at increasingly higher orders of perturbation theory, determine the quark and gluon distributions in the proton. Modern QCD fit procedures use data sets from a number of different experiments to determine the x dependence of the PDFs at some initial scale Q_0^2 . By evolution a complete description of the data considered is achieved in a χ^2 minimisation procedure which considers correlations among the experimental data points [2].

This traditional extraction procedure has some drawbacks and challenges. Firstly, the number of input data sets, in particular in global analyses, is large. Data points are correlated through common systematic uncertainties, both within and across the data sets. These correlations are not always fully documented and handling the experimental data without additional expert knowledge can become difficult. Secondly, the treatment of the systematic error correlations is not unique.

In the Lagrange multiplier or Hessian method [3] each systematic error source is treated as an additional fit parameter with a quadratic penalty term included in the χ^2 definition to penalise large deviations of the source from the nominal experimentally determined value. The parameters are fitted assuming that the data model, as provided by (N)NLO QCD, will then optimise the experimental systematic error sources as well as constrain the PDF parameters. Error propagation is used to estimate the resulting uncertainties on the PDFs. This procedure is considered legal if the systematic error parameters are moved in the fit by not more than about one standard deviation. Larger discrepancies may indicate a deficiency in the underlying theoretical model. In the so-called “offset” method (see e.g. [4, 5]) the data sets are shifted in turn by the effect of each single systematic error before fitting. The resulting fits are then used to form an envelope function as an estimate of the PDF uncertainty. Each method has its own advantages and shortcomings, and there is no agreed standard.

All analyses face the problem of data sets not always leading to consistent results and sometimes not agreeing well. Some global QCD analyses thus use non-statistical criteria to estimate the PDF uncertainties ($\Delta\chi^2 = T^2 \gg 1$). The size of T^2 is set to ensure that all input data sets are consistent with the result of the global fit at a 90% confidence level. The H1 and ZEUS data, with a few exceptions, cover the same kinematic range. It is thus possible to check that the measurements of the two collaborations agree within errors which is indeed the case.¹

The drawbacks mentioned can be significantly reduced by averaging the cross section data in a model independent way prior to performing a QCD analysis of that data. The present paper introduces such a method, based on ref. [6] and applies it to the HERA I data. In this method one fit parameter is included for each unique cross section measurement at a given (x, Q^2, y) value, and represents the averaged value of the cross section at that kinematic point.

¹Some HERA I low Q^2 NC data sets have been observed to have different normalisation by about 3% which is about a 2σ disagreement. A reanalysis of the H1 luminosity measurement of the special minimum bias run in 1997 has led to a change in integrated luminosity. After correction, the H1 minimum bias data below Q^2 of 12 GeV² have moved up by +3.4% which is taken into account in the present combination.

3 Combination Method

The only theoretical input to the present averaging procedure is the assumption that the ZEUS and H1 experiments are measuring the same cross sections at the same kinematic points. The correlated systematic uncertainties are floated coherently such that each experiment calibrates the other one. This allows a significant reduction of the correlated systematic uncertainty for much of the kinematic plane. In addition, a study of the global χ^2/dof of the average and of the pull distributions provides a model independent consistency check between the experiments.

The probability distribution of a measurement quantity M for a single data set can be represented as a χ^2 function

$$\chi_{\text{exp}}^2 (M^{i,\text{true}}, \alpha_j) = \sum_i \frac{\left[M^{i,\text{true}} - \left(M^i + \sum_j \frac{\partial M^i}{\partial \alpha_j} \alpha_j \right) \right]^2}{\delta_i^2} + \sum_j \frac{\alpha_j^2}{\delta_{\alpha_j}^2}. \quad (1)$$

Here M^i are the measured central values, and δ_i the statistical and uncorrelated systematic uncertainties, of the quantity M . The $M^{i,\text{true}}$ are their true values; α_j are parameters for the j sources of correlated systematic uncertainty and $\partial M^i / \partial \alpha_j$ denotes the sensitivity of point i to source j . For the cross section measurements the index i labels a particular measurement at a given (x, Q^2) . Eq. 1 represents the correlated probability distribution functions for the quantity $M^{i,\text{true}}$ and for the systematic uncertainties α_j .

The χ^2 function of Eq. 1 has by construction a minimum $\chi^2 = 0$ for $M^{i,\text{true}} = M^i$ and $\alpha_j = 0$. The total uncertainty for $M^{i,\text{true}}$ determined from the formal minimisation of Eq. 1 is equal to the quadratic sum of the statistical and systematic uncertainties. The covariance matrix $\text{cov}(M^{i,\text{true}}, M^{j,\text{true}})$ quantifies the correlation between the experimental points.

In the analysis of more than one data set, a total χ^2 function, χ_{tot}^2 , is built from the sum of the χ^2 functions for each data set. The χ_{tot}^2 function can be minimised with respect to $M^{i,\text{true}}$ and α_j ; this minimisation corresponds to a generalisation of the averaging procedure which takes correlations between different data sets into account. The quantity χ_{tot}^2 is a sum of positive definite quadratic functions so that it is itself a positive definite quadratic function and thus has a unique minimum which can be found as a solution of a system of linear equations. Although this system of equations has a large dimension, it can be accurately and quickly solved.

The χ^2 function of Eq. 1 is most suitable for measurements in which the uncertainties are absolute or *additive*, i.e. do not depend on the central value of the measurement. For the cross section measurements, however, the correlated and uncorrelated systematic errors are proportional to the central values. This proportionality can be approximated by a linear dependence. In this case the combination of the data sets using Eq. 1 has a bias towards lower cross section values since the measurements with smaller central values have smaller absolute uncertainties. An improved χ^2 definition is given by

$$\chi_{\text{exp}}^2 (M^{i,\text{true}}, \alpha_j) = \sum_i \frac{\left[M^{i,\text{true}} - \left(M^i + \sum_j \frac{\partial M^i}{\partial \alpha_j} \frac{M^{i,\text{true}}}{M^i} \alpha_j \right) \right]^2}{\left(\delta_i \frac{M^{i,\text{true}}}{M^i} \right)^2} + \sum_j \frac{\alpha_j^2}{\delta_{\alpha_j}^2}, \quad (2)$$

in which the relative or *multiplicative* uncertainties for each measurement are translated to the absolute ones using $M^{i,\text{true}}$ values which are common for all measurements. It has been verified numerically using a toy Monte Carlo technique that this definition of the χ^2 function does not lead to a systematic bias for an average of a set of measurements with the same relative uncertainties.

Unlike Eq. 1, the χ^2 function Eq. 2 is not a simple quadratic form with respect to $\{M^{i,\text{true}}\}, \{\alpha_j\}$. The minimum is found by an iterative procedure: first Eq. 1 is used to get an initial approximation for $\{M^{i,\text{true}}\}$, next all the errors are recalculated using $\delta_i \rightarrow \frac{M^{i,\text{true}}}{M^i} \delta_i$ and the minimisation is repeated. Convergence is observed after two iterations.

After the minimisation the systematic uncertainties are shifted with respect to the original central values and they are correlated with each other. To simplify the usage of the average and to preserve the original form of the χ^2 definition, Eq. 2, the covariance matrix of the systematic uncertainties is diagonalised and the uncertainties are redefined such that the expectation values are set to 0 and the standard deviations are set to 1.

The combined data set of deep inelastic scattering (DIS) cross section measurements from HERA-I which is obtained here following Eq. 2 retains the full correlations between data points. This averaging method removes the drawback of the offset method, where the size of the systematic uncertainties is fixed.

4 Data Treatment

The data used for the combination consist of the published double differential unpolarised NC and CC cross section measurements of H1 and ZEUS taken in the years 1994 – 2000 and are listed in Tab.1. During this period HERA operated with a proton beam energy, E_p , of 820 GeV until 1997, and 920 GeV from 1998 onwards. The Q^2 range in this combination covers $1.5 - 30\,000 \text{ GeV}^2$ and an x coverage from $6 \times 10^{-5} - 0.65$ which corresponds to a range of inelasticity $y = Q^2/(sx)$ between about 0.8 and 0.007. Here s is the centre-of-mass energy squared, $s = 4E_e E_p$, and E_e was equal to about 27.5 GeV. These data are the most precise data published by both collaborations to date.

Note that there are data available for Q^2 below 1 GeV^2 , both from shifted vertex operation and from ZEUS using a dedicated detector near the beam pipe. These data have not been considered here, but will be included in subsequent data combination analyses.

The double differential cross section measurements are published with their statistical and systematic uncertainties. The statistical uncertainties are uncorrelated between different data points. The systematic uncertainties are classified into three sub-categories: (i) point-to-point uncorrelated uncertainties e.g. statistical errors due to the Monte Carlo event simulation. These uncertainties are added quadratically to the statistical uncertainties defining a total point-to-point uncorrelated uncertainty; (ii) point-to-point correlated uncertainties, for example electromagnetic and hadronic energy scale calibration uncertainties; (iii) an overall normalisation uncertainty of the various data sets. Sources of point-to-point correlated uncertainties are often common for CC and NC cross section measurements and sometimes can be considered to be

data set		x range		Q^2 range (GeV ²)		\mathcal{L} pb^{-1}	comment	ref.
H1 NC min. bias	97	0.00008	0.02	3.5	12	1.8	$e^+p \sqrt{s} = 301$ GeV	[7]
H1 NC low Q^2	96 – 97	0.000161	0.20	12	150	17.9	$e^+p \sqrt{s} = 301$ GeV	[7]
H1 NC	94 – 97	0.0032	0.65	150	30 000	35.6	$e^+p \sqrt{s} = 301$ GeV	[4]
H1 CC	94 – 97	0.013	0.40	300	15 000	35.6	$e^+p \sqrt{s} = 301$ GeV	[4]
H1 NC	98 – 99	0.0032	0.65	150	30 000	16.4	$e^-p \sqrt{s} = 319$ GeV	[8]
H1 CC	98 – 99	0.013	0.40	300	15 000	16.4	$e^-p \sqrt{s} = 319$ GeV	[8]
H1 NC	99 – 00	0.00131	0.65	100	30 000	65.2	$e^+p \sqrt{s} = 319$ GeV	[9]
H1 CC	99 – 00	0.013	0.40	300	15 000	65.2	$e^+p \sqrt{s} = 319$ GeV	[9]
ZEUS NC	96 – 97	0.00006	0.65	2.7	30 000	30.0	$e^+p \sqrt{s} = 301$ GeV	[10]
ZEUS CC	94 – 97	0.015	0.42	280	17 000	47.7	$e^+p \sqrt{s} = 301$ GeV	[11]
ZEUS NC	98 – 99	0.005	0.65	200	30 000	15.9	$e^-p \sqrt{s} = 319$ GeV	[12]
ZEUS CC	98 – 99	0.015	0.42	280	30 000	16.4	$e^-p \sqrt{s} = 319$ GeV	[13]
ZEUS NC	99 – 00	0.005	0.65	200	30 000	63.2	$e^+p \sqrt{s} = 319$ GeV	[14]
ZEUS CC	99 – 00	0.008	0.42	280	17 000	60.9	$e^+p \sqrt{s} = 319$ GeV	[15]

Table 1: Table of H1 and ZEUS data sets used in the averaging procedure. The integrated luminosity of each data set (\mathcal{L}) is given as well as the kinematic ranges in x and Q^2 .

correlated for different data sets of the same experiment. They are treated as independent between H1 and ZEUS, since a correlation arising from the beam energy uncertainties assumed in the kinematic reconstruction and calibration, is negligible. Similarly, the normalisation uncertainties are correlated for all cross section measurements by a given experiment from a common data taking period.

All the NC and CC cross section data from H1 and ZEUS are combined in one simultaneous minimisation. Therefore resulting shifts of correlated systematic uncertainties and global normalisations propagate coherently to both CC and NC data.

4.1 Extrapolation to the common $x - Q^2$ binning

Prior to the combination, the H1 and ZEUS data are transformed to a common grid of x, Q^2 points. The transformation of a measurement from the given x, Q^2 to the nearby x_{grid}, Q^2_{grid} on the grid is performed using a straightforward interpolation formula

$$\sigma_{NC,CC}^{e^{\pm}p}(x_{grid}, Q^2_{grid}) = \frac{\sigma_{NC,CC}^{th,e^{\pm}p}(x_{grid}, Q^2_{grid})}{\sigma_{NC,CC}^{th,e^{\pm}p}(x, Q^2)} \sigma_{NC,CC}^{e^{\pm}p}(x, Q^2). \quad (3)$$

The grid points are chosen such that the interpolation corrections are minimal taking advantage of the fact that the original x, Q^2 grids of H1 and ZEUS are not too different. Furthermore, the chosen grid ensures that no two separate measurements of the same data set interpolate to a common grid point. The majority of the H1 and ZEUS measurements are averaged to one single common data point. However, for some of the grid points there is no nearby counter part from the other experiment giving points in the combined cross section which originate from either H1 or ZEUS only. Note that through the treatment of the systematic error correlations, such data points may be shifted with respect to the original measurement in the averaging procedure.

The H1 parameterisation of the double differential NC and CC cross sections (H1PDF2000) was used for the extrapolations to the common $x - Q^2$ grid. To check the sensitivity to this cross section parameterisation, the ZEUS-JETS parameterisation [5] was also used. The resulting correction factors agreed to a few permille for the NC and to better than 2% for the CC cross sections. These differences are negligible compared to the experimental uncertainty.

4.2 Centre of Mass Energy Correction

In the data sets considered there are subsamples from $E_p = 820$ GeV and from 920 GeV. The cross sections, both for NC and CC scattering, depend weakly on the energy via terms containing the inelasticity y , besides depending on x and Q^2 . Thus there is a choice to be made of obtaining one common data set at a single centre-of-mass energy, or keeping the results for the two proton beam energies separate. At the present stage of the data combination, to ease comparison with theoretical predictions and illustrate the main features of the method introduced here, the 820 GeV high Q^2 data are corrected to 920 GeV and then combined with the genuine measurements at $E_p = 920$ GeV, both for charged and neutral currents. For the CC data the correction is calculated as

$$\sigma_{CC}^{e^\pm p}_{920}(x, Q^2) = \sigma_{CC}^{e^\pm p}_{820}(x, Q^2) \frac{\sigma_{CC}^{th, e^\pm p}_{920}(x, Q^2)}{\sigma_{CC}^{th, e^\pm p}_{820}(x, Q^2)} \quad (4)$$

For NC data the correction is performed additively as

$$\sigma_{NC}^{e^\pm p}_{920}(x, Q^2) = \sigma_{NC}^{e^\pm p}_{820}(x, Q^2) + \Delta\sigma_{NC}^{e^\pm p}(x, Q^2, y_{920}, y_{820}). \quad (5)$$

The correction term is sizable only at large y and calculated as the difference between H1 PDF2000 based predictions of the DIS cross sections with $y_{920} = Q^2/(4x E_e 920)\tilde{\text{GeV}}$ and $y_{820} = Q^2/(4x E_e 820)\tilde{\text{GeV}}$

$$\Delta\sigma_{NC}^{e^\pm p}(x, Q^2, y_{920}, y_{820}) = F_L(x, Q^2) \left[\frac{y_{820}^2}{Y_{820}^+} - \frac{y_{920}^2}{Y_{920}^+} \right] + xF_3(x, Q^2) \left[\pm \frac{Y_{820}^-}{Y_{820}^+} \mp \frac{Y_{920}^-}{Y_{920}^+} \right], \quad (6)$$

where $Y_\pm = 1 \pm (1 - y^2)$. To estimate the uncertainty on the combined data arising from the centre-of-mass energy correction another average is performed assuming $F_L = 0$ as an extreme assumption in the correction. The difference between this average and the usual procedure using the H1PDF2000 prediction for F_L is an estimate of the systematic uncertainty. The uncertainty is found to be at the permille level across most of the kinematic plane, and only reaching 5% for very few points at $y > 0.6$. This uncertainty is added in quadrature to the combined data. In forthcoming analyses the centre-of-mass energy correction will be limited to values of $y < 0.35$ and for larger y the 820 and 920 GeV proton beam energy data will be kept separate. This will limit the size of the additional systematic error to below 0.5%.

4.3 Additive vs Multiplicative Error Treatment

The central values for the combined H1 and ZEUS cross sections are extracted as the $M^{i, \text{true}}$ values using Eq. 2. The fact that the normalisation uncertainties are relative (multiplicative) in nature has been discussed in the literature [16] and is generally agreed by the community however, for the other systematic uncertainties the situation is not so clear. Some groups consider both correlated and uncorrelated systematic uncertainties to be additive [17], while others consider correlated uncertainties as multiplicative and uncorrelated uncertainties as additive [9].

To assess the sensitivity of the average to this issue, various different treatments of the systematic uncertainties are considered. The extreme assumptions treat all uncertainties as multiplicative, Eq. 2, or all as additive, apart from the normalisation uncertainties. An additional systematic uncertainty is estimated based on the difference between these two error treatments. The typical size of this uncertainty is $< 1\%$ for the low Q^2 data reaching $1 - 1.5\%$ for the larger Q^2 data. This uncertainty is presently added as an additional point-to-point correlated source of uncertainty on the averaged cross sections.

4.4 Correlation of the H1 and ZEUS Systematic Uncertainties

The H1 and ZEUS Collaborations use similar methods to reconstruct the event kinematics, employ similar techniques for the detector calibration, use common Monte Carlo simulation models for the hadronic final state simulation as well as for photoproduction background subtraction. This similarity of approaches and techniques may lead to correlations between H1 and ZEUS measurements.

In practice only a small part of these correlations can be easily identified. Part of the normalisation uncertainty is correlated across all data sets and experiments arising from a small contribution of 0.5% due to uncertain higher order QED corrections to the Bethe-Heitler process used in luminosity measurements by both experiments. A second clear example arises from the uncertainty of higher order electroweak radiative corrections in DIS. This leads to a 0.5% correlation between experiments in the point-to-point uncorrelated error. Aside from these two cases the measurements of H1 and ZEUS are assumed to be uncorrelated.

To estimate the sensitivity to this assumption, 12 pairs of systematic uncertainties of common origin (γp background, electromagnetic and hadronic energy scale, electron scattering angle) for various calorimeters in H1 and ZEUS (SpaCal and LAr calorimeters in H1 and FCAL, BCAL and RCAL in ZEUS) are selected to be 100% correlated. Then $2^{12} - 1$ different averages are calculated assuming each of the 12 pairs to be correlated or uncorrelated in turn and these alternative averages are compared to the central average for which all sources are assumed to be uncorrelated. This investigation shows that the average values are rather insensitive to the assumptions on correlation between the two experiments. The largest effect on the average have differing assumptions on the γp background (a $1 - 2\%$ change at $y > 0.6$ for low $Q^2 < 20 \text{ GeV}^2$) and on the hadronic energy calibration (1% at low $y < 0.02$). For these sources the measurements rely more on the simulation of the hadronic final state which is similar for the two experiments. These variations are therefore introduced as additional point-to-point correlated systematic sources of uncertainty of the averaged cross sections.

5 Results

In this minimisation procedure 1153 individual NC and CC measurements are averaged to 554 unique points. This yields a good quality of fit with the $\chi^2/dof = 510/599$. The distribution of pulls does not show any significant tensions across the kinematic plane. A total of 43 sources of correlated systematic uncertainty are considered in this analysis. With the exception of the

H1 normalisation for the 96 – 97 low Q^2 data [7], all other error sources lie within 1σ of the nominal values from the published data. The H1 96 – 97 normalisation is moved by 1.6σ corresponding to a shift of $+2.6\%$. Almost all systematic uncertainties are reduced, with the most significant reductions observed for the H1 backward calorimeter energy scale by a factor of three, and the ZEUS uncertainty of modelling forward hadronic energy flow by a factor of four. In the region $Q^2 < 60 \text{ GeV}^2$ the published H1 and ZEUS data each have a precision of $\sim 2-3\%$ which is dominated by the systematic uncertainties. In comparison the combined data set reaches a precision of $\simeq 1.5\%$. At higher Q^2 more substantial improvements in uncertainty are achieved, although this is largely due to a reduction in the statistical uncertainty.

The combined data for NC e^+p scattering are shown in Fig.1 and Fig.2 from $Q^2 = 1.5 - 30\,000 \text{ GeV}^2$. At the highest Q^2 the combined data have a significantly reduced total uncertainty of order 10% which is driven by the increased statistical accuracy which dominates the measurement error. A similar comparison is shown in Fig.3 for the high Q^2 e^-p scattering data. In all figures, the data are shown in comparison to two previously published QCD fits performed by each experiment on their own data sets. As expected the fits continue to provide an excellent description of the data.

The complete e^+p NC data are shown again in Fig.4 spanning the entire x and Q^2 range demonstrating the scaling violations at both high and low x . In Fig.5 a close up in linear scale of three x bins is shown as a function of Q^2 . The combined data are compared to the individual measurements from H1 and ZEUS (shifted for clarity). At low Q^2 where the data are limited by systematic uncertainties, the improvement in the total error is visible. At higher Q^2 the combined data exhibit far smaller fluctuations as compared to the published data.

In Fig.6 and Fig.7 the combined HERA CC e^+p and e^-p scattering data are shown respectively. The e^+p data correspond to a total integrated luminosity of approximately 200 pb^{-1} and have a typical precision of $\sim 8\%$, whereas the e^-p data with approximately 30 pb^{-1} , have a precision of $\sim 20\%$. Again, in both cases the two NLO QCD fits provide a good description of the data.

6 Summary

A new model independent method of combining cross section measurements has been presented in which a coherent treatment of systematic uncertainties allows a substantial reduction in the total errors. The method has been demonstrated on the complete set of published HERA I structure function data. High statistics data from the HERA II running period are being analysed by the two collaborations and will be included in subsequent combination analyses devoted to precision determinations of the parton distributions in the proton.

Acknowledgements

We are grateful to the HERA machine group whose outstanding efforts have made this experiment possible. We thank the engineers and technicians for their work in constructing and maintaining the H1 and ZEUS detectors, our funding agencies for financial support, the DESY technical staff for continual assistance and the DESY directorate for support and for the hospitality which they extend to the non DESY members of the collaboration.

HERA I e^+p Neutral Current Scattering - H1 and ZEUS

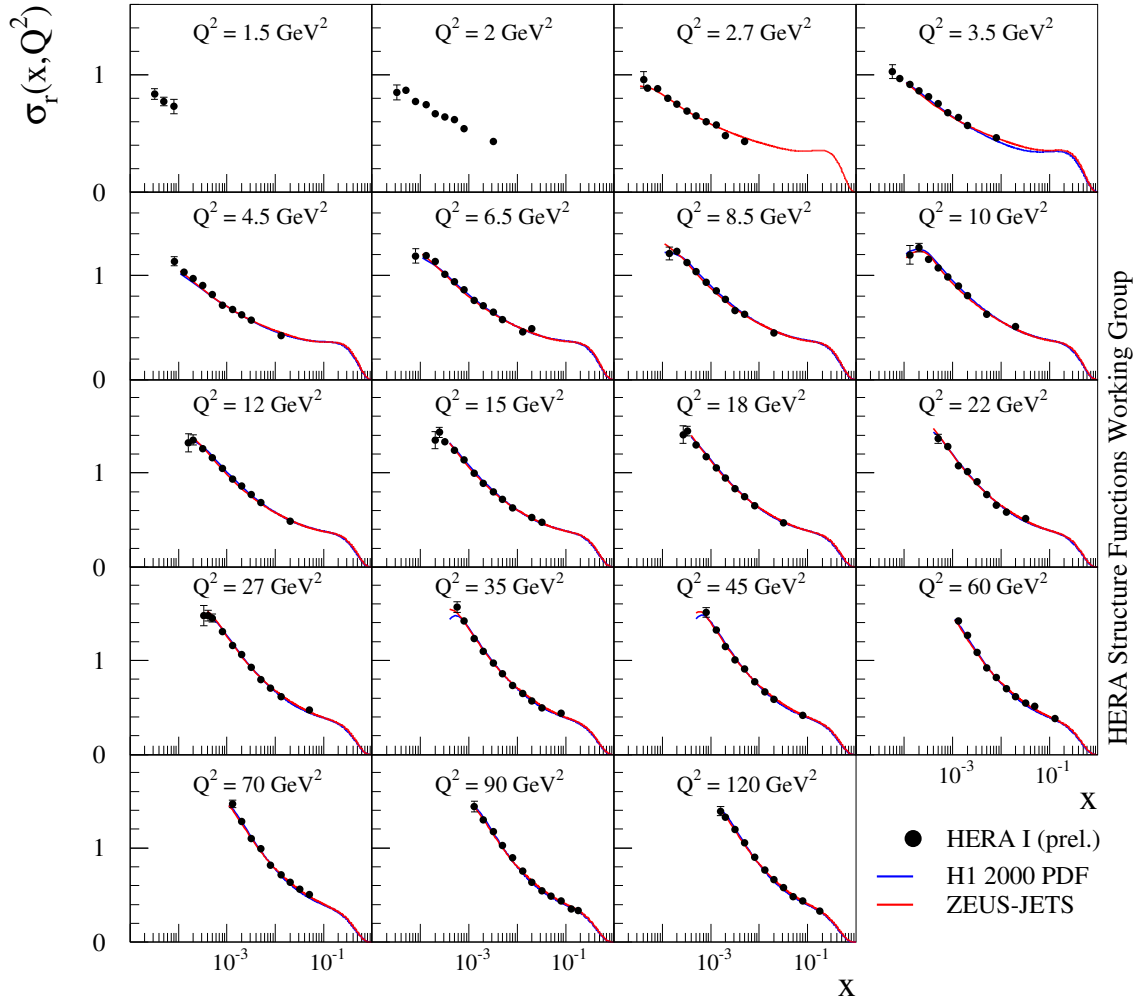


Figure 1: Deep inelastic neutral current e^+p scattering cross section for lower Q^2 , 1.5 – 120 GeV^2 , obtained from the combination of published HERA I measurements by H1 and ZEUS. The curves are NLO QCD fits as performed by H1 and ZEUS to their own data, shown for $Q^2 \geq Q_{min}^2$ as chosen in the fit procedure.

HERA I e^+p Neutral Current Scattering - H1 and ZEUS

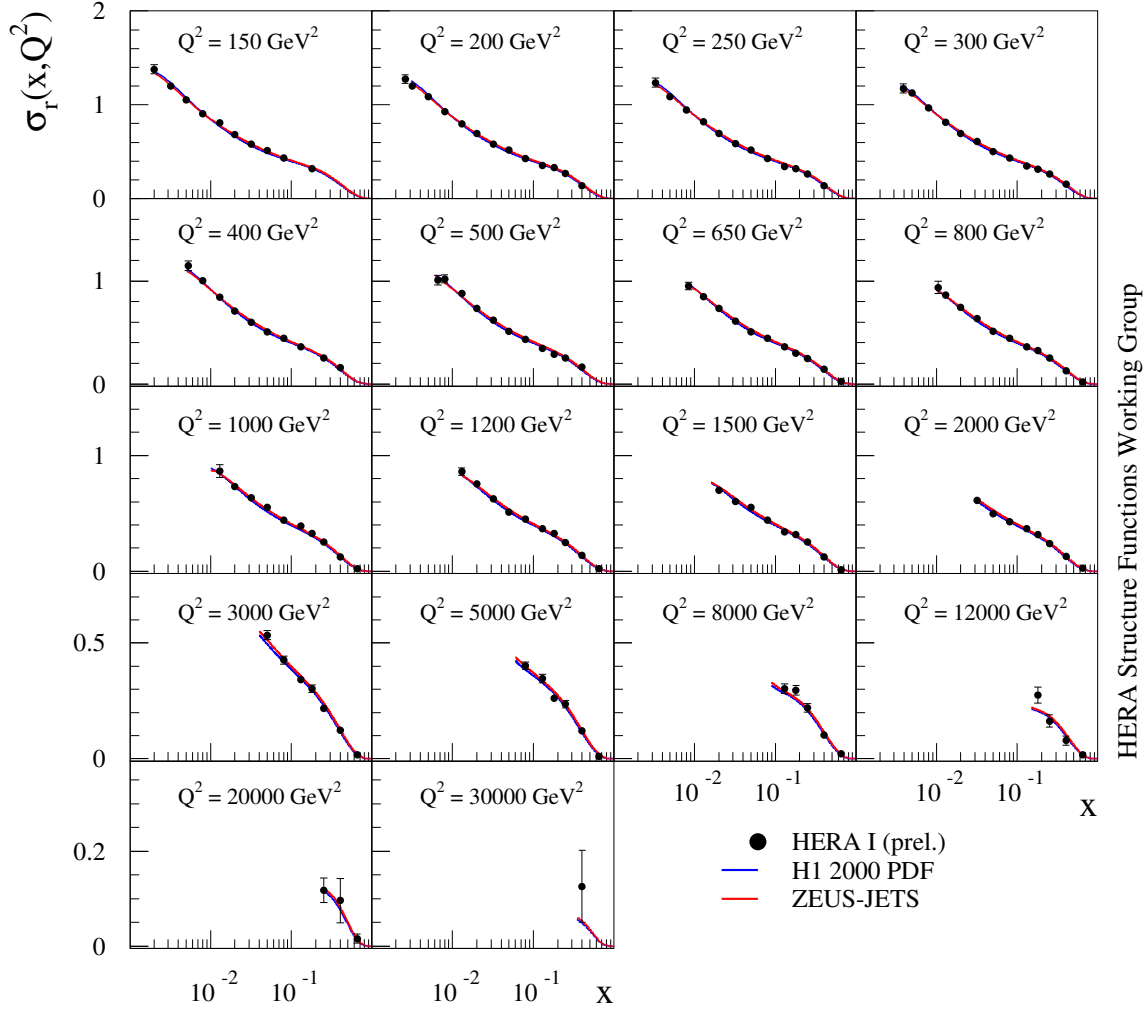


Figure 2: Deep inelastic neutral current e^+p scattering cross section for high Q^2 , 150 – 30000 GeV^2 , obtained from the combination of published HERA I measurements by H1 and ZEUS. The curves are NLO QCD fits as performed by H1 and ZEUS to their own data.

HERA I e^-p Neutral Current Scattering - H1 and ZEUS

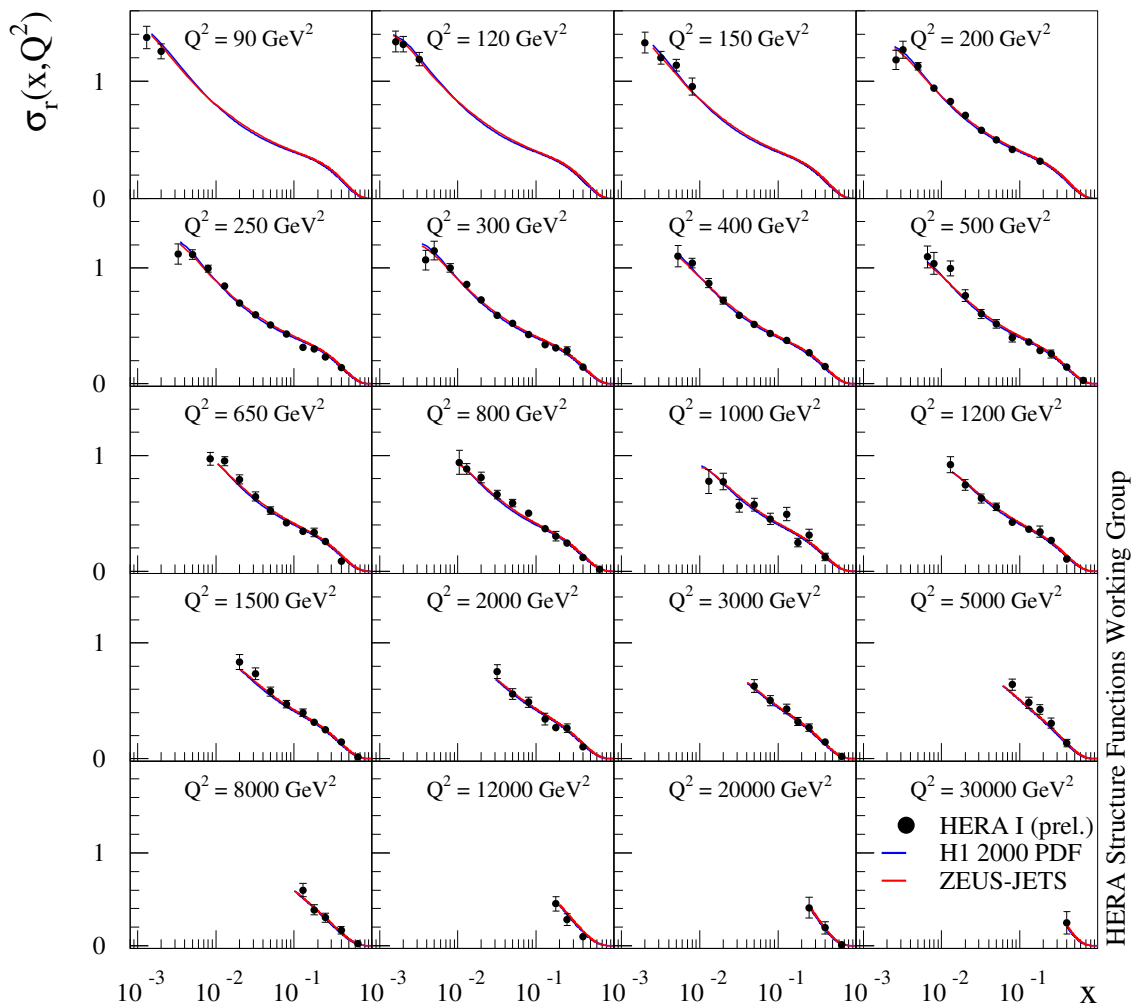


Figure 3: Deep inelastic neutral current e^-p scattering cross section for high Q^2 , 90 – 30000 GeV^2 , obtained from the combination of published HERA I measurements by H1 and ZEUS. The curves are NLO QCD fits as performed by H1 and ZEUS to their own data.

HERA I e^+p Neutral Current Scattering - H1 and ZEUS

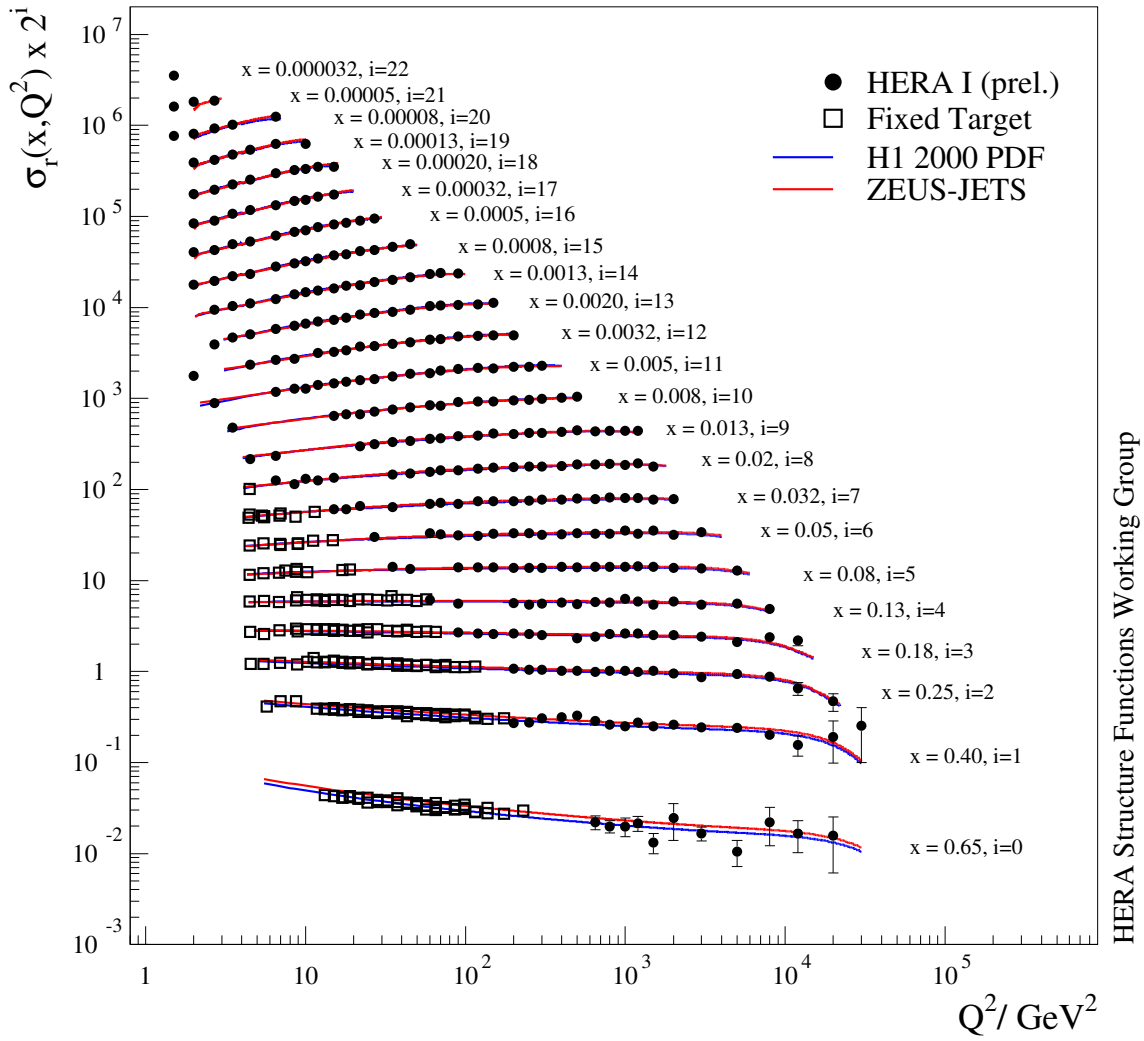


Figure 4: Deep inelastic neutral current e^+p scattering cross section data from the HERA I data taking period as obtained by combining the published H1 and ZEUS measurements. The curves are NLO QCD fits as performed by H1 and ZEUS to their own data.

HERA I e^+p Neutral Current Scattering - H1 and ZEUS

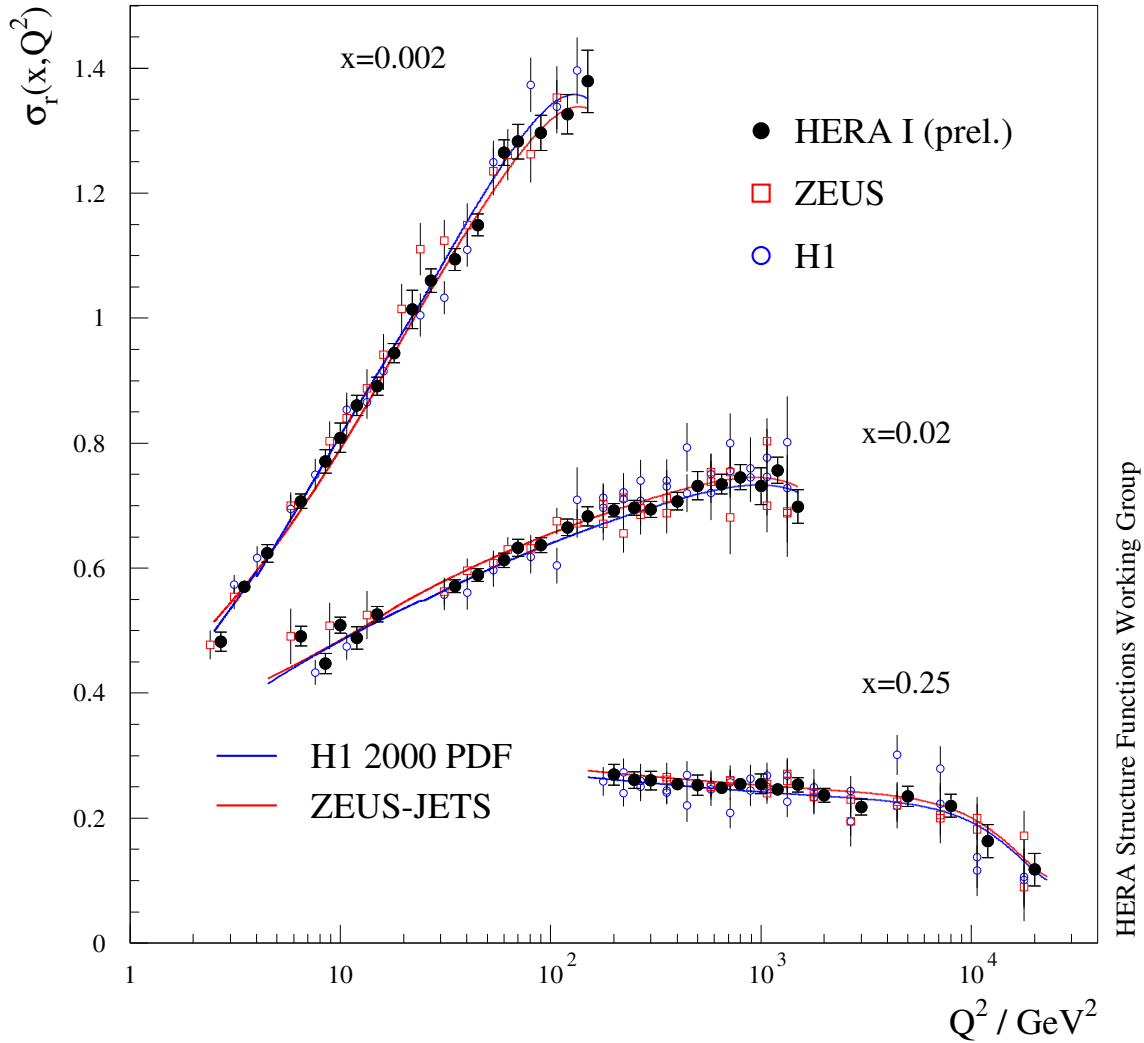


Figure 5: Deep inelastic neutral current e^+p scattering cross section measurements for three selected x bins as a function of Q^2 . The H1 (open points) and ZEUS data (open squares) are compared to the H1 and ZEUS combined data (open points). Measurements from the individual experiments have been shifted for clarity. The error bars show the total uncertainty. The curves are NLO QCD fits as performed by H1 and ZEUS to their own data.

HERA I e^+p Charged Current Scattering - H1 and ZEUS

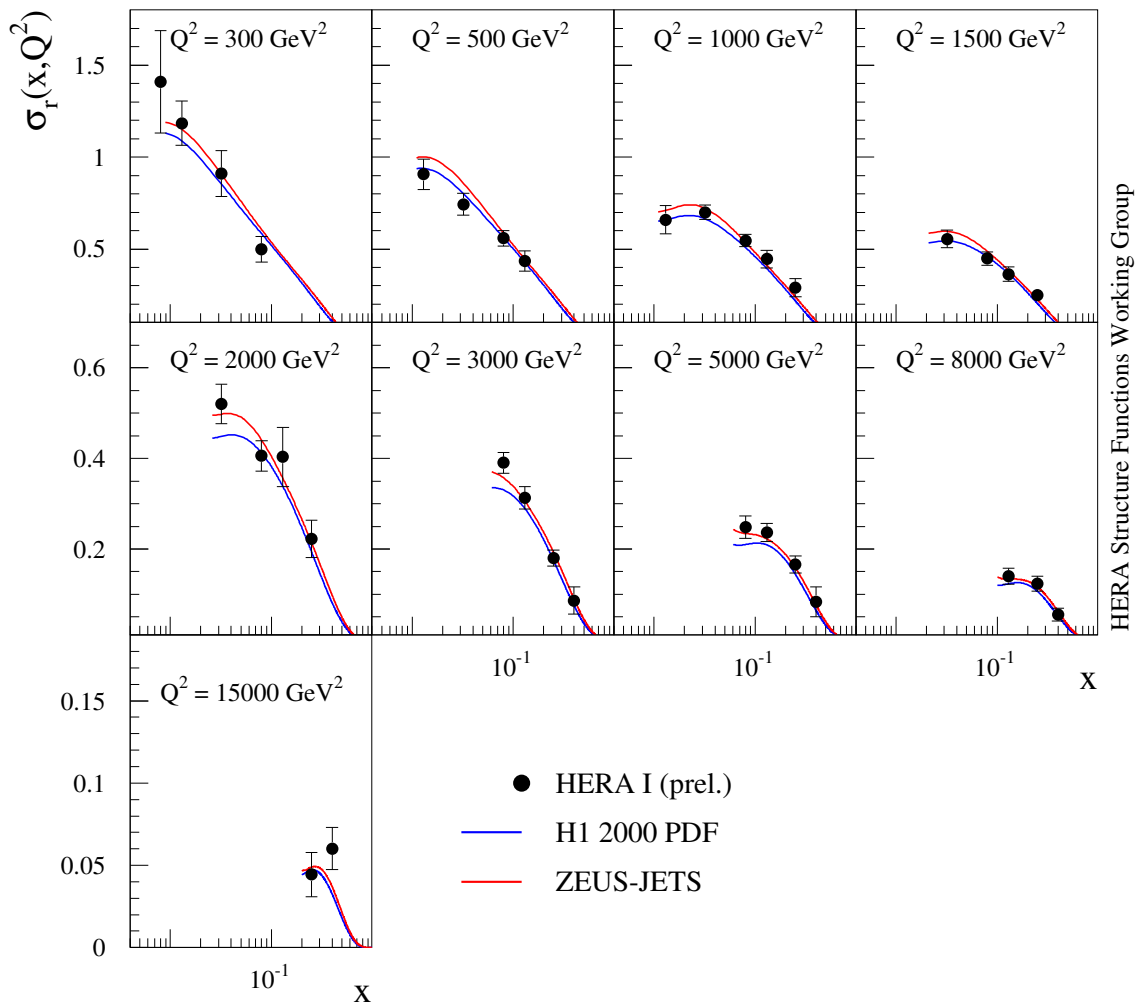


Figure 6: Deep inelastic charged current e^+p scattering cross section for Q^2 between 300 and 15 000 GeV^2 , obtained from the combination of the measurements by H1 and ZEUS as published from data taken in HERA I. The curves are NLO QCD fits as performed by H1 and ZEUS to their own data.

HERA I e^-p Charged Current Scattering - H1 and ZEUS

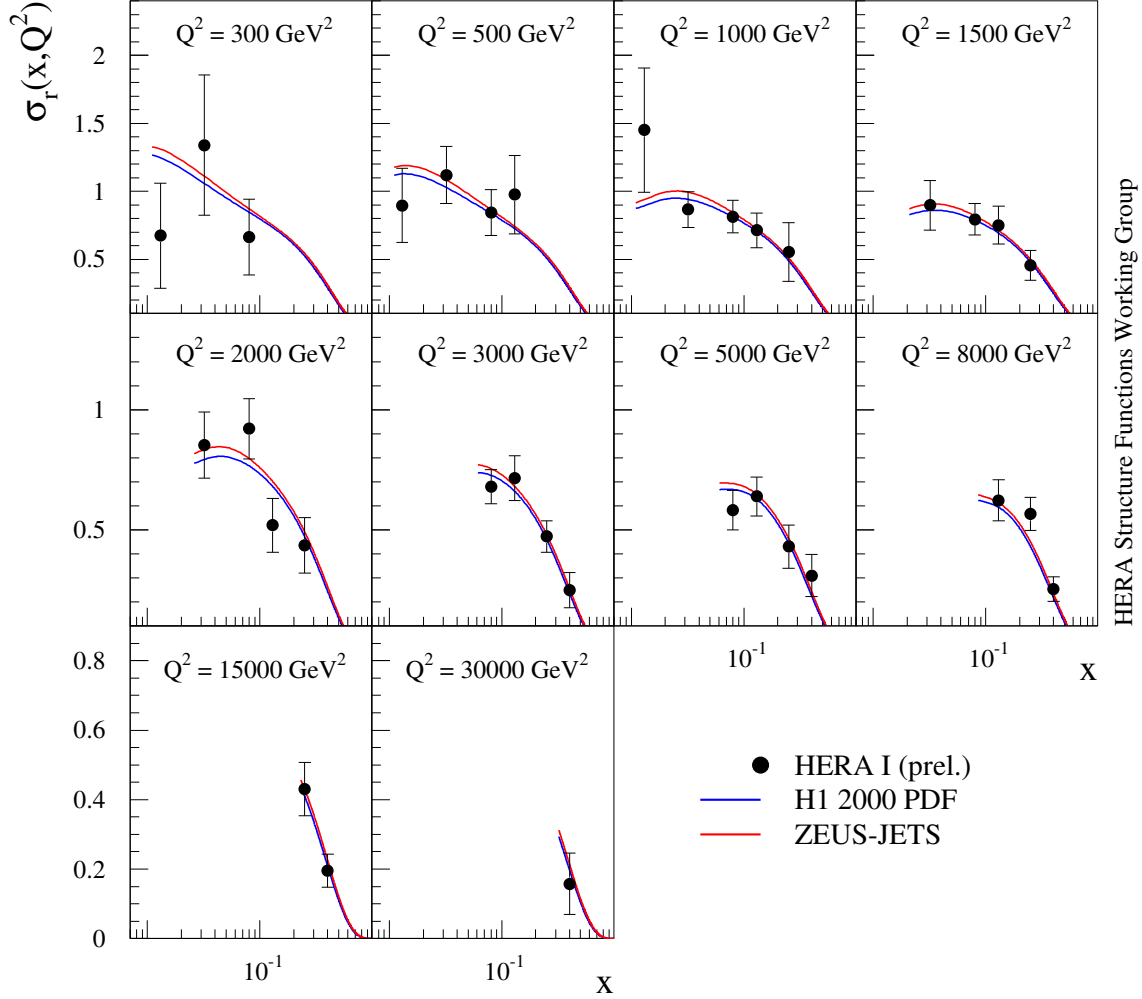


Figure 7: Deep inelastic charged current e^-p scattering cross section for Q^2 between 300 and 30 000 GeV^2 , obtained from the combination of the measurements by H1 and ZEUS as published from data taken in HERA I. The curves are NLO QCD fits as performed by H1 and ZEUS to their own data.

References

- [1] [H1 and ZEUS Collaborations] H1 prelim-06-142, ZEUS prelim-06-022, XXXIII International Conference on High Energy Physics Moscow, Russia, July 2006.
- [2] R. Devenish and A. Cooper-Sarkar, *OUP. (2004) Ch. 6*
- [3] C. Pascaud and F. Zomer, LAL preprint, LAL/95-05 (1995),
C. Pascaud and F. Zomer, hep-ph/0104013.
- [4] C. Adloff *et al.* [H1 Collaboration], *Eur. Phys. J. C* **13** (2000) 609 [hep-ex/9908059].
- [5] S. Chekanov *et al.* [ZEUS Collaboration], *Eur. Phys. J. C* **42** (2005) 1 [hep-ph/0503274].
- [6] S. Glazov XIII International Workshop on Deep Inelastic Scattering
Wisconsin, USA, April 2005.
- [7] C. Adloff *et al.* [H1 Collaboration], *Eur. Phys. J. C* **21** (2001) 33 [hep-ex/0012053].
- [8] C. Adloff *et al.* [H1 Collaboration], *Eur. Phys. J. C* **19** (2001) 269 [hep-ex/0012052].
- [9] C. Adloff *et al.* [H1 Collaboration], *Eur. Phys. J. C* **30** (2003) 1 [hep-ex/0304003].
- [10] S. Chekanov *et al.* [ZEUS Collaboration], *Eur. Phys. J. C* **21** (2001) 443 [hep-ex/0105090].
- [11] J. Breitweg *et al.* [ZEUS Collaboration], *Eur. Phys. J. C* **12** (2000) 411 [Erratum-ibid. C **27** (2003) 305] [hep-ex/9907010].
- [12] S. Chekanov *et al.* [ZEUS Collaboration], *Eur. Phys. J. C* **28** (2003) 175 [hep-ex/0208040].
- [13] S. Chekanov *et al.* [ZEUS Collaboration], *Phys. Lett. B* **539** (2002) 197 [Erratum-ibid. B **552** (2003) 308] [hep-ex/0205091].
- [14] S. Chekanov *et al.* [ZEUS Collaboration], *Phys. Rev. D* **70** (2004) 052001 [hep-ex/0401003].
- [15] S. Chekanov *et al.* [ZEUS Collaboration], *Eur. Phys. J. C* **32** (2003) 1 [hep-ex/0307043].
- [16] S. Alekhin, *JETP Lett.* **82** (2005) 628 [*Pisma Zh. Eksp. Teor. Fiz.* **82** (2005) 710] [hep-ph/0508248].
- [17] W. K. Tung *et al.* *JHEP* **0702** (2007) 053 [hep-ph/0611254].